

See discussions, stats, and author profiles for this publication at: <https://www.researchgate.net/publication/321763570>

A new high-resolution chronology for the late Maastrichtian warming event: Establishing robust temporal links with the...

Article in *Geology* · December 2017

DOI: 10.1130/G39771.1

CITATIONS

0

READS

84

7 authors, including:



Dick Kroon

The University of Edinburgh

949 PUBLICATIONS 8,413 CITATIONS

[SEE PROFILE](#)



Thomas Westerhold

Universität Bremen

127 PUBLICATIONS 2,133 CITATIONS

[SEE PROFILE](#)



Ursula Röhl

MARUM Center for Marine Environmental Scien...

324 PUBLICATIONS 9,654 CITATIONS

[SEE PROFILE](#)



J.C. Zachos

University of California, Santa Cruz

670 PUBLICATIONS 24,030 CITATIONS

[SEE PROFILE](#)

Some of the authors of this publication are also working on these related projects:



A single age model for all equatorial Pacific ocean drilling sites. [View project](#)



Surface and Mediterranean Outflow Water Dynamics in the Gulf of Cadiz during the Pleistocene (MOWCADYN) [View project](#)

1 A new high-resolution chronology for the late Maastrichtian
2 warming event: Establishing robust temporal links with the
3 onset of Deccan volcanism

4 **James S.K. Barnet¹, Kate Littler¹, Dick Kroon², Melanie J. Leng³, Thomas Westerhold⁴,**
5 **Ursula Röhl⁴ and James C. Zachos⁵**

6 *¹Camborne School of Mines & Environment and Sustainability Institute, University of Exeter,*
7 *Penryn Campus, Cornwall, TR10 9FE, UK*

8 *²School of Geosciences, University of Edinburgh, Edinburgh, EH9 3JW, UK*

9 *³NERC Isotope Geosciences Laboratory, British Geological Survey, Nottingham, NG12 5GG,*
10 *UK and Centre for Environmental Geochemistry, University of Nottingham, Nottingham, NG7*
11 *2RD, UK*

12 *⁴MARUM, University of Bremen, Leobener Strasse, 28359, Bremen, Germany*

13 *⁵Department of Earth and Planetary Sciences, University of California Santa Cruz, 1156 High*
14 *Street, Santa Cruz, California, 95064, USA*

15

16 **ABSTRACT**

17 The late Maastrichtian warming event was defined by a global temperature increase of
18 about 2.5–5°C, which occurred ~150–300 kyr before the K/Pg (Cretaceous/Paleogene) mass
19 extinction. This transient warming event has traditionally been associated with a major pulse of
20 Deccan Trap volcanism, however, large uncertainties associated with radiogenic dating methods
21 have long hampered a definitive correlation. Here we present a new high-resolution, single-
22 species, benthic stable isotope record from the South Atlantic, calibrated to an updated orbitally-

23 tuned age model, to provide a revised chronology of the event, which we then correlate to the
24 latest radiogenic dates of the main Deccan Trap eruption phases. Our data reveals that the
25 initiation of deep-sea warming coincides, within uncertainty, with the onset of the main phase of
26 Deccan volcanism, strongly suggesting a causal link. The onset of deep-sea warming is
27 synchronous with a 405-kyr eccentricity minimum, excluding a control by orbital forcing alone,
28 although amplified carbon cycle sensitivity to orbital precession is evident during the greenhouse
29 warming. A more precise understanding of Deccan-induced climate change paves the way for
30 future work focusing on the fundamental role of these precursor climate shifts in the K/Pg mass
31 extinction.

32

33 **INTRODUCTION**

34 A period of rapid climate change, represented initially by a transient global warming event and
35 followed by a global cooling, occurred during the last few hundred thousand years of the
36 Maastrichtian and may have played an ancillary role in the ultimate demise of many terrestrial
37 and marine biota at the K/Pg (Cretaceous/Paleogene) boundary (e.g. Keller et al., 2016). The so-
38 called “late Maastrichtian warming event” was characterized by a transient global $\sim 2.5\text{--}4^\circ\text{C}$
39 warming in the marine realm based on benthic $\delta^{18}\text{O}$ and organic paleothermometer ($\text{TEX}_{86}^{\text{H}}$) data
40 (e.g. Li & Keller, 1998; Woelders et al., 2017), and $\sim 5^\circ\text{C}$ warming in the terrestrial realm based
41 on pedogenic carbonate $\delta^{18}\text{O}$ and proportion of untoothed leaf margins in woody dicot plants
42 (Nordt et al., 2003; Wilf et al., 2003). Enhanced deep-sea carbonate dissolution, most
43 pronounced in the high latitudes (Henehan et al., 2016), and abrupt decreases in vertical
44 temperature and carbon isotope gradients in the marine water column have also been
45 documented (Li & Keller, 1998).

46 This transient warming event has previously been linked to a major pulse of Deccan Trap
47 volcanism, centered in modern day western India, however, until recently the large uncertainties
48 associated with radiogenic dating have hampered a robust correlation (e.g. Chenet et al., 2007).
49 In recent years improvements in precision of radiogenic dating methods have allowed for a more
50 robust correlation between pre-K/Pg climate change and volcanism (e.g. Renne et al., 2015;
51 Schoene et al., 2015). To complement advances in dating of the volcanic sequences, here we
52 present the highest resolution (1.5–4 kyr), complete single-species benthic stable isotope record
53 produced to date, calibrated to an updated orbitally-tuned age model, for the final million years
54 of the Maastrichtian and first 500 kyr of the Danian. This allows us to much more accurately
55 correlate the major climatic shifts of the terminal Maastrichtian with Deccan volcanism,
56 facilitating future work investigating the link between Deccan-induced climate change and the
57 K/Pg mass extinction.

58

59 **MATERIALS AND METHODS**

60 A stratigraphically continuous late Maastrichtian–early Danian sedimentary section was
61 recovered at Ocean Drilling Program (ODP) Site 1262 (Walvis Ridge, South Atlantic;
62 27°11.15'S, 1°34.62'E; water depth 4759 m, Maastrichtian water depth ~3000 m, (Shipboard
63 Scientific Party, 2004)), where the late Maastrichtian is represented by an expanded section of
64 foraminifera-bearing, carbonate-rich nannofossil ooze with a mean sedimentation rate of 1.5–2
65 cm/kyr. We have constructed an updated orbitally-tuned age model for this site based on
66 recognition of the stable 405-kyr eccentricity cycle in our high-resolution benthic carbon isotope
67 ($\delta^{13}\text{C}_{\text{benthic}}$) dataset, correlated to the La2010b solution of Laskar et al. (2011) and anchored to an
68 astronomical K/Pg boundary age of 66.02 Ma (Dinarès-Turell et al., 2014). The key tie points

69 used to create the portion of the age model considered here are listed in Table DR2 in the Data
70 Repository. All existing published data presented herein has also been migrated over to the same
71 age model for comparison (Figs. 1, 2; detailed methods provided in the Data Repository). We
72 generated $\delta^{13}\text{C}$ and $\delta^{18}\text{O}$ data using the epifaunal benthic foraminifera species *Nuttallides*
73 *truempyi* on an IsoPrime 100 Gas Source Isotope Ratio Mass Spectrometer in dual inlet mode
74 equipped with a Multiprep device at the NERC Isotope Geosciences Facility (British Geological
75 Survey). The internal standard, KCM, calibrated against the international standard NBS-19, was
76 used to place data on the VPDB scale, with average sample analytical precision (1σ) of 0.03‰
77 for $\delta^{13}\text{C}$ and 0.05‰ for $\delta^{18}\text{O}$. The complete benthic stable isotope data set is available online in
78 the PANGAEA database doi.pangaea.de/10.1594/PANGAEA.881019. Bottom water
79 temperatures were calculated from $\delta^{18}\text{O}_{\text{benthic}}$ data by converting *N. truempyi* data to *Cibicidoides*
80 values, then using Equation 1 of Bemis et al. (1998). Stable isotope data was graphically
81 detrended in KaleidaGraph 4.0 using a 15% running mean, to remove long-term trends, then
82 band pass filtering was conducted in AnalySeries 2.0 (Paillard et al., 1996) for 405-kyr
83 eccentricity at 0.002467 +/- 0.000700 cycles/kyr and 100-kyr eccentricity at 0.010 +/- 0.003
84 cycles/kyr.

85

86 **RESULTS**

87 The new stable isotope data shows relatively stable and cool temperatures persisted in the deep
88 South Atlantic Ocean from 67.1–66.8 Ma, followed by the onset of a longer term gradual
89 warming (1°C) and decline in $\delta^{13}\text{C}_{\text{benthic}}$ values from 66.75–66.5 Ma (Fig. 1). The late
90 Maastrichtian warming event initiated at ~66.34 Ma, just over 300 kyr before the K/Pg
91 boundary, with peak warming of ~+4°C ($\delta^{18}\text{O}_{\text{benthic}}$ excursion of ~-0.8‰) attained between

92 ~66.27–66.18 Ma (Fig. 1). A more gradual, step-wise cooling to pre-excursion temperatures then
93 took place over the next 200 kyr, terminating at the K/Pg boundary (Fig. 1). Conversely, the
94 $\delta^{13}\text{C}_{\text{benthic}}$ record appears to show a muted response compared to the $\delta^{18}\text{O}_{\text{benthic}}$ record during the
95 warming event, with only a minor negative excursion of $\sim 0.5\text{‰}$ noted between 66.3–66.2 Ma
96 (Fig. 1). The magnitude and character of the excursions in $\delta^{13}\text{C}_{\text{benthic}}$ and $\delta^{18}\text{O}_{\text{benthic}}$ data at Site
97 1262 are similar to those reported in lower resolution data from Deep Sea Drilling Project
98 (DSDP) Site 525 (Li & Keller, 1998; Fig. DR3), located at a shallower paleo-depth of 1–1.5 km
99 on Walvis Ridge, suggesting a similar magnitude of warming in deep and intermediate waters of
100 the South Atlantic. Confirming that these characteristics are global, deep Pacific stable isotope
101 data from ODP Site 1209 also show a coeval but somewhat smaller warming pulse, and a similar
102 muted response in $\delta^{13}\text{C}_{\text{benthic}}$ values to those observed in the Atlantic (Fig. 2; Westerhold et al.,
103 2011). The minor offset of Pacific $\delta^{13}\text{C}_{\text{benthic}}$ values by up to -0.4‰ relative to the South Atlantic,
104 suggests an older water mass was bathing the equatorial Pacific site, consistent with previously
105 reported Paleocene–Eocene trends (Littler et al., 2014; Fig. 2). The onset of the warming event in
106 the Atlantic corresponds to a 405-kyr eccentricity minimum, with the peak of the event occurring
107 during a 100 kyr eccentricity maximum but prior to a 405-kyr eccentricity maximum. The
108 $\delta^{18}\text{O}_{\text{benthic}}$ leads $\delta^{13}\text{C}_{\text{benthic}}$ (i.e. climate leads carbon cycle) by $\sim 30\text{--}40$ kyr within the 405-kyr
109 band, consistent with Late Paleocene–Early Eocene trends recorded further upsection at this site
110 (Littler et al., 2014). Interestingly, the $\delta^{18}\text{O}_{\text{benthic}}$ and $\delta^{13}\text{C}_{\text{benthic}}$ data become antiphase at the 100-
111 kyr frequency during the warming event, but are in phase with carbon lagging oxygen by ~ 10
112 kyr earlier in the Maastrichtian and by ~ 5 kyr during the earliest Danian (Fig. 1).

113

114 **DISCUSSION**

115 The new high-resolution, benthic stable isotope data placed onto our updated orbitally-tuned age
116 model demonstrates that the late Maastrichtian warming event closely coincides with the onset of
117 the main phase of Deccan volcanism, irrespective of radiogenic dating technique used, strongly
118 suggesting a causal link (Fig. 1). Furthermore, both the relatively long duration of the warming
119 event and the initiation of the warming during a minimum in the 405-kyr eccentricity cycle
120 suggest a control by orbital forcing alone is unlikely, and that Deccan volcanogenic CO₂
121 emissions were likely to be the primary climate driver over 100-kyr timescales. Based on the
122 distribution of red boles (weathering horizons) within the Deccan basalts, volcanism of the pre-
123 K/Pg Kalsubai sub-group was characterized by more frequent eruptions of a smaller magnitude,
124 likely leading to a larger cumulative atmospheric *p*CO₂ increase than post-K/Pg eruptions (Renne
125 et al., 2015; Schoene et al., 2015). By contrast, Danian eruptions had longer hiatuses between
126 large eruptive events, allowing for partial CO₂ sequestration by silicate weathering or organic
127 burial.

128 Despite the strong evidence for climatic warming and somewhat sparse evidence for elevated
129 atmospheric *p*CO₂ (Barclay & Wing, 2016; Nordt et al., 2002, 2003; Fig. 1), characteristic of
130 many hyperthermals of the early Paleogene such as the Paleocene Eocene Thermal Maximum
131 (PETM; e.g. McInerney & Wing, 2011), the C isotope records and lack of evidence for
132 significant ocean acidification at Site 1262 (e.g., reduction in %CaCO₃ or increase in Fe
133 concentration) suggest a relatively minor C-cycle perturbation (Figs. 1; 2). Given the
134 comparatively heavy δ¹³C signature (−7‰) of volcanogenic CO₂, voluminous Deccan emissions
135 may not have created a major perturbation to the isotope composition of the global δ¹³C pool.
136 The absence of a major negative carbon cycle perturbation suggests that sources of isotopically-
137 light carbon (e.g. biogenic methane or the oxidation of organic matter), were not destabilized and

138 released in significant quantities during the event. This differential response between the
139 $\delta^{18}\text{O}_{\text{benthic}}$ and $\delta^{13}\text{C}_{\text{benthic}}$ records, and the lack of evidence for significant global deep-ocean
140 acidification (Fig. 1), may be due to rates of volcanogenic CO_2 emission and consequent
141 background–peak warming, which occurred rather slowly over ~70–80 kyr during the late
142 Maastrichtian event, but was much more rapid, on the order of 10–20 kyr, during Paleogene
143 hyperthermals (e.g., McInerney and Wing, 2011; Zeebe et al., 2017). However, evidence for
144 enhanced deep-sea dissolution during this event has been described from the high-latitudes in
145 % CaCO_3 records from ODP Site 690 (Henehan et al., 2016) and in orbitally-tuned Fe intensity
146 and magnetic susceptibility data from IODP Site U1403 on the Newfoundland margin
147 (Batenburg et al., 2017). These deep-sea sites may have been particularly sensitive to smaller
148 carbon cycle perturbations during this time, with Site 690 located in the principle region of deep
149 water formation in the Southern Ocean and with Site U1403, situated at a paleodepth of ~4 km,
150 being more sensitive to smaller fluctuations in the Maastrichtian Calcite Compensation Depth
151 than the shallower Site 1262 (Henehan et al., 2016). Clearly, more high-resolution pCO_2 proxy
152 studies are urgently required to more confidently assess Deccan-induced perturbations to the
153 global carbon cycle. The lag between the climate and carbon cycle response within the 405-kyr
154 band (Fig. 1), as seen throughout the Paleocene–Eocene (Littler et al., 2014), may suggest that
155 small quantities of light carbon were released as a positive feedback to orbitally-driven warming.
156 The observed antiphase behavior between $\delta^{13}\text{C}$ and $\delta^{18}\text{O}$ within the 100 kyr band during the
157 warming event, but not before or after (Fig. 1), may result from the pulsed release of small
158 amounts of isotopically-light carbon superimposed on the longer (300 kyr) scale warming
159 imparted by the Deccan eruptions. Additionally, amplified precession scale (~21 kyr) variability
160 visible in the dissolution proxies (Fe and % CaCO_3) and $\delta^{13}\text{C}$ records during the event, also

161 suggest increased carbon-cycle sensitivity, perhaps due to generally elevated CO₂ levels from
162 Deccan activity (Fig. 1).
163 The limited available planktic stable isotope data (e.g., ODP Site 690) suggests significant
164 warming, on the order of ~2.5°C, occurred in the southern high latitudes during the event (Fig. 2;
165 Stott & Kennett, 1990). Organic paleothermometer TEX₈₆^H data from the Neuquén Basin,
166 Argentina, also suggests significant warming of surface waters of ~3°C in continental shelf
167 settings at mid-latitudes (Fig. 1; Woelders et al., 2017). Recently, a negative bulk δ¹⁸O excursion
168 of 1‰ has also been resolved from the Newfoundland margin, suggesting a pronounced surface
169 water warming also occurred in the mid-northern latitudes during this time, although bulk δ¹⁸O
170 values cannot reliably be converted into absolute surface water temperatures (Batenburg et al.,
171 2017). By contrast, there appears to have been very little change in surface water temperatures at
172 lower latitudes, although this interpretation is tentative based on the availability of only one fine
173 fraction data set from DSDP Site 577 (Fig. 2). A much more significant bottom water warming at
174 mid–low latitudes created a dramatic reduction in the surface–deep temperature gradient and
175 reduced thermal stratification of the water column (Li & Keller, 1998; Fig. 2). Taken together,
176 this data suggests a possible polar amplification of surface water warming during the late
177 Maastrichtian warming event, but clearly, more single-species planktic isotope records over a
178 greater latitudinal coverage are required to fully evaluate latitudinal variations in surface
179 temperature during this event.

180

181 **CONCLUSIONS**

182 Our revised chronology for the late Maastrichtian warming event, combined with the latest
183 radiogenic dates for Deccan volcanism, point to the synchronous onset of the main phase of

184 Deccan volcanism with the late Maastrichtian warming event ~300 kyr before the K/Pg
185 boundary. The onset of the warming is unlikely to have been orbitally controlled, further
186 supporting volcanic CO₂ as the trigger. Increased carbon cycle sensitivity to orbital precession is
187 evident during the greenhouse event suggesting system sensitivity to background temperature
188 conditions. Now that the environmental effects of Deccan volcanism have been more confidently
189 established, future work should focus on evaluating the role of these precursor climatic changes
190 in the K/Pg mass extinction.

191
192 Figure 1. Correlation of environmental proxies to Deccan volcanism and the La2010b orbital
193 solution. A. Recalibrated atmospheric *p*CO₂ estimates based on pedogenic carbonate (purple
194 triangles; raw data from Nordt et al., 2002, recalibrated in this study) and stomatal indices
195 (orange circles; Beerling et al., 2002, recalibrated by Barclay & Wing, 2016; green circles;
196 Steinthorsdottir et al., 2016). B. New benthic δ¹³C and δ¹⁸O data from Site 1262 and filters at the
197 405-kyr and 100-kyr bands (this study), correlated to the La2010b solution (Laskar et al., 2011),
198 TEX₈₆^H data (Woelders et al., 2017) and Site 1262 Fe and %CaCO₃ data (Kroon et al., 2007).
199 Error bars on TEX₈₆^H data represent analytical uncertainty (dark green) and calibration error of
200 absolute temperatures (pale green). Magnetozones from Bowles (2006) and nannozones from
201 Shipboard Scientific Party (2004), with high-resolution K/Pg biozones from Bernaola &
202 Monechi (2007). C. Timing of Deccan volcanism, with formation volumes calculated by the
203 equal area method (grey), variable area method (red), and red bole distribution illustrated as a
204 black line, using Ar-Ar ages in Renne et al. (2015). U-Pb age data from Schoene et al. (2015)
205 also shown. See Data Repository for detailed methods.

206

207 Figure 2. Stable isotope data across the late Maastrichtian event. A. Benthic $\delta^{13}\text{C}$ & $\delta^{18}\text{O}$ data for
208 Site 1262 (this study) plotted against benthic data from Site 1209 (equatorial Pacific; Westerhold
209 et al., 2011) for comparison. B. Planktic $\delta^{13}\text{C}$ & $\delta^{18}\text{O}$ data from Site 577, equatorial Pacific
210 (Zachos et al., 1985), Site 525, South Atlantic (Li & Keller, 1998) and Site 690, Southern Ocean
211 (Stott & Kennett, 1990). Planktic and bulk $\delta^{18}\text{O}$ data has been normalized to a baseline of 0‰
212 for pre-event conditions to compare the magnitude of the warming event by latitude. C. Shallow-
213 to-deep $\delta^{13}\text{C}$ and temperature gradients at Site 525 (Li & Keller, 1998).

214

215 **ACKNOWLEDGMENTS**

216 The new Site 1262 $\delta^{13}\text{C}$ and $\delta^{18}\text{O}$ data were funded by the NERC Isotope Geosciences Facility at
217 the British Geological Survey (IP-1581-1115), and we also thank Hilary Sloane for technical
218 support. We thank the Bremen Core Repository for allowing us to collect the required samples
219 and Gerta Keller for providing the raw stable isotope data from Site 525. Financial support for
220 this research was provided by the Deutsche Forschungsgemeinschaft (DFG) to Ursula Röhl and
221 Thomas Westerhold.

222

223 **REFERENCES CITED**

224 Barclay, R.S., and Wing, S.L., 2016, Improving the Ginkgo CO_2 barometer: Implications for the
225 early Cenozoic atmosphere: *Earth and Planetary Science Letters*, v. 439, p. 158–171, doi:
226 10.1016/j.epsl.2016.01.012.

227 Batenburg, S.J., Friedrich, O., Moriya, K., Voigt, S., Cournède, C., Moebius, I., Blum, P.,
228 Bornemann, A., Fiebig, J., Hasegawa, T., Hull, P.M., Norris, R.D., Röhl, U., Sexton, P.F.,
229 Westerhold, T., Wilson, P.A., and the IODP Expedition 342 Scientists, 2017, Late

230 Maastrichtian carbon isotope stratigraphy and cyclostratigraphy of the Newfoundland
231 Margin (Site U1403, IODP Leg 342): Newsletters on Stratigraphy (in press), doi:
232 10.1127/nos/2017/0398.

233 Beerling, D.J., Lomax, B.H., Royer, D.L., Upchurch, G.R., and Kump, L.R., 2002, An
234 atmospheric pCO₂ reconstruction across the Cretaceous-Tertiary boundary from leaf
235 megafossils: Proceedings of the National Academy of Sciences of the United States of
236 America, v. 99, p. 7836–7840, doi: 10.1073/pnas.122573099.

237 Bemis, B.E., Spero, H.J., Bijma, J., and Lea, D.W., 1998, Reevaluation of the oxygen isotopic
238 composition of planktonic foraminifera: Experimental results and revised paleotemperature
239 equations: Paleoceanography, v. 13, p. 150–160, doi: 10.1029/98PA00070.

240 Bernaola, G., and Monechi, S., 2007, Calcareous nannofossil extinction and survivorship across
241 the Cretaceous-Paleogene boundary at Walvis Ridge (ODP Hole 1262C, South Atlantic
242 Ocean): Palaeogeography, Palaeoclimatology, Palaeoecology, v. 255, p. 132–156, doi:
243 10.1016/j.palaeo.2007.02.045.

244 Bowles, J., 2006, Data report: revised magnetostratigraphy and magnetic mineralogy of
245 sediments from Walvis Ridge, Leg 208. In Kroon, D., Zachos, J.C., and Richter, C. (Eds.),
246 Proc. ODP, Sci. Results, 208: College Station, TX (Ocean Drilling Program), 1–24,
247 doi:10.2973/odp.proc.sr.208.206.2006.

248 Chenet, A.L., Quidelleur, X., Fluteau, F., Courtillot, V., and Bajpai, S., 2007, ⁴⁰K-⁴⁰Ar dating of
249 the Main Deccan large igneous province: Further evidence of KTB age and short duration:
250 Earth and Planetary Science Letters, v. 263, p. 1–15, doi: 10.1016/j.epsl.2007.07.011.

251 Dinarès-Turell, J., Westerhold, T., Pujalte, V., Röhl, U., and Kroon, D., 2014, Astronomical
252 calibration of the Danian stage (Early Paleocene) revisited: Settling chronologies of

253 sedimentary records across the Atlantic and Pacific Oceans: *Earth and Planetary Science*
254 *Letters*, v. 405, p. 119–131, doi: 10.1016/j.epsl.2014.08.027.

255 Henehan, M.J., Hull, P.M., Penman, D.E., Rae, J.W.B., and Schmidt, D.N., 2016,
256 Biogeochemical significance of pelagic ecosystem function: an end-Cretaceous case study:
257 *Philosophical Transactions of the Royal Society B: Biological Sciences*, v. 371, p. 1-10, doi:
258 10.1098/rstb.2015.0510.

259 Keller, G., Punekar, J., and Mateo, P., 2016, Upheavals during the Late Maastrichtian:
260 Volcanism, climate and faunal events preceding the end-Cretaceous mass extinction:
261 *Palaeogeography, Palaeoclimatology, Palaeoecology*, v. 441, p. 137–151, doi:
262 10.1016/j.palaeo.2015.06.034.

263 Kroon, D., Zachos, J.C., and Leg 208 Scientific Party, 2007, Leg 208 Synthesis: Cenozoic
264 climate cycles and excursions: *Proceedings of the Ocean Drilling Program, Scientific*
265 *Results*, v. 208, p. 1-55, doi: 10.2973/odp.proc.sr.208.201.2007.

266 Laskar, J., Fienga, A., Gastineau, M., and Manche, H., 2011, La2010: a new orbital solution for
267 the long-term motion: *Astronomy & Astrophysics*, v. 532 (A89), p. 1–15,
268 doi.org/10.1051/0004-6361/201116836.

269 Li, L., and Keller, G., 1998, Abrupt deep-sea warming at the end of the Cretaceous: *Geology*, v.
270 26, p. 995-998, doi: 10.1130/0091-7613(1998)026<0995:ADSWAT>2.3.CO;2.

271 Littler, K., Röhl, U., Westerhold, T., and Zachos, J.C., 2014, A high-resolution benthic stable-
272 isotope record for the South Atlantic: Implications for orbital-scale changes in Late
273 Paleocene-Early Eocene climate and carbon cycling: *Earth and Planetary Science Letters*, v.
274 401, p. 18–30, doi: 10.1016/j.epsl.2014.05.054.

275 McInerney, F.A., and Wing, S.L., 2011, The Paleocene-Eocene Thermal Maximum: A
276 Perturbation of Carbon Cycle, Climate, and Biosphere with Implications for the Future:
277 Annual Review of Earth & Planetary Sciences, v. 39, p. 489–516, doi: 10.1146/annurev-
278 earth-040610-133431.

279 Nordt, L., Atchley, S., and Dworkin, S.I., 2002, Paleosol barometer indicates extreme
280 fluctuations in atmospheric CO₂ across the Cretaceous-Tertiary boundary: *Geology*, v. 30, p.
281 703–706, doi: 10.1130/0091-7613(2002)030<0703:PBIEFI>2.0.CO;2.

282 Nordt, L., Atchley, S., and Dworkin, S., 2003, Terrestrial evidence for two greenhouse events in
283 the latest Cretaceous: *GSA Today*, v. 13, p. 4–9, doi: 10.1130/1052-
284 5173(2003)013<4:TEFTGE>2.0.CO;2.

285 Paillard, D., Labeyrie, L., and Yiou, P., 1996, Macintosh program performs time-series analysis.
286 EOS Transactions AGU77, v. 77, p. 379, doi: 10.1029/96EO00259.

287 Renne, P.R., Sprain, C.J., Richards, M.A., Self, S., Vanderkluysen, L., and Pande, K., 2015,
288 State shift in Deccan volcanism at the Cretaceous-Paleogene boundary, possibly induced by
289 impact: *Science*, v. 350, p. 76–78, doi: 10.1126/science.aac7549.

290 Schoene, B., Samperton, K.M., Eddy, M.P., Keller, G., Adatte, T., Bowring, S.A., Khadri,
291 S.F.R., and Gertsch, B., 2015, U-Pb geochronology of the Deccan Traps and relation to the
292 end-Cretaceous mass extinction: *Science*, v. 347, p. 182–184, doi: 10.1126/science.aaa0118.

293 Shipboard Scientific Party, 2004, Site 1262, in Zachos, J.C., Kroon, D., Blum, P., et al.,
294 Proceedings of the Ocean Drilling Program, Initial Reports, Volume 208: College Station,
295 TX (Ocean Drilling Program), p. 1-92, doi: 10.2973/odp.proc.ir.208.103.2004.

296 Steinthorsdottir, M., Vajda, V., and Pole, M., 2016, Global trends of pCO₂ across the
297 Cretaceous–Paleogene boundary supported by the first Southern Hemisphere stomatal

298 proxy-based pCO₂ reconstruction: *Palaeogeography, Palaeoclimatology, Palaeoecology*, v.
299 464, p. 143–152, doi: 10.1016/j.palaeo.2016.04.033.

300 Stott, L.D., and Kennett, J.P., 1990, The paleoceanographic and paleoclimatic signature of the
301 Cretaceous/Paleogene boundary in the Antarctic : stable isotopic results from ODP leg 113.:
302 *Proceedings of the Ocean Drilling Program (Barker P.F., Kennett J.P., et al.)*, Scientific
303 Results, 113, p. 829-848.

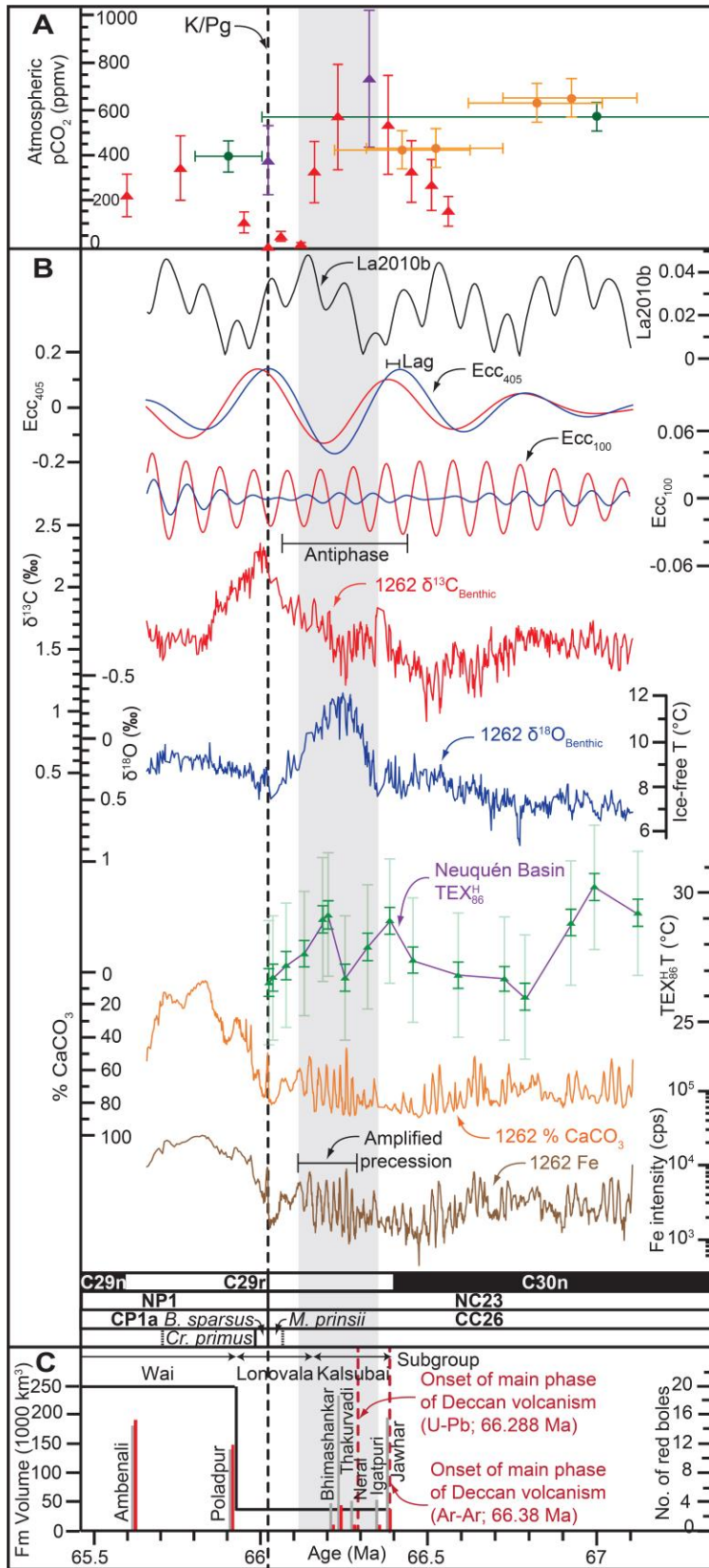
304 Westerhold, T., Röhl, U., Donner, B., Mccarren, H.K., and Zachos, J.C., 2011, A complete high-
305 resolution Paleocene benthic stable isotope record for the central Pacific (ODP Site 1209):
306 *Paleoceanography*, v. 26, p. 1–13, doi: 10.1029/2010PA002092.

307 Wilf, P., Johnson, K.R., and Huber, B.T., 2003, Correlated terrestrial and marine evidence for
308 global climate changes before mass extinction at the Cretaceous-Paleogene boundary:
309 *Proceedings of the National Academy of Sciences of the United States of America*, v. 100,
310 p. 599–604, doi: 10.1073/pnas.0234701100.

311 Woelders, L., Vellekoop, J., Kroon, D., Smit, J., 2017, Casadio, S., Prámparo, M.B., Dinarès-
312 Turell, J., Peterse, F., Sluijs, A., and Speijer, R.P. Latest Cretaceous climatic and
313 environmental change in the South Atlantic region: *Paleoceanography*, v. 32, p. 466-483,
314 doi: 10.1002/2016PA003007.

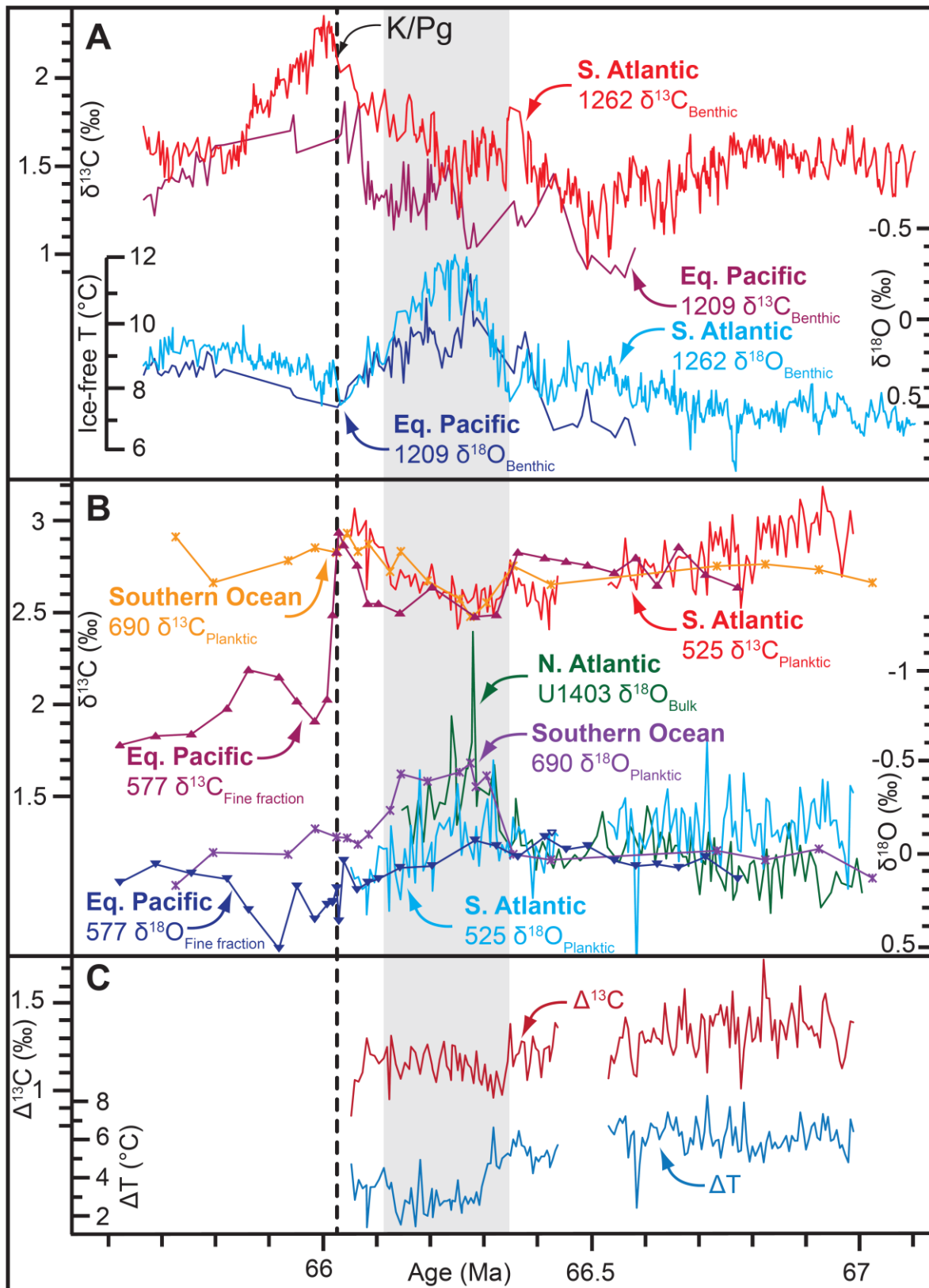
315 Zachos, J.C., Arthur, M.A., Thunell, R.C., Williams, D.F., and Tappa, E.J., 1985, Stable isotope
316 and trace element geochemistry of carbonate sediments across the Cretaceous/Tertiary
317 Boundary at Deep Sea Drilling Project Hole 577, Leg 86.: *Initial Reports of the Deep Sea
318 Drilling Project*, 86, p. 513–532, doi:10.2973/dsdp.proc.86.120.1985.

319 Zeebe, R.E., Westerhold, T., Littler, K., and Zachos, J.C., 2017, Orbital Forcing of the Paleocene
320 and Eocene Carbon Cycle: *Paleoceanography*, v. 32, p. 440-465, doi:
321 10.1002/2016PA003054.



322

323 Figure 1.



324
325
326

Figure 2.